

## Charged–Higgs effects in a new $B \rightarrow D\tau\nu_\tau$ differential decay distribution

Ulrich Nierste, Stéphanie Trine, and Susanne Westhoff

*Institut für Theoretische Teilchenphysik  
Karlsruhe Institute of Technology, 76128 Karlsruhe, Germany*

We show that the decay mode  $B \rightarrow D\tau\nu_\tau$  is competitive with and complementary to  $B \rightarrow \tau\nu_\tau$  in the search for charged–Higgs effects. Updating the relevant form factors, we find that the differential distribution in the decay chain  $\bar{B} \rightarrow D\bar{\nu}_\tau\tau^- [\rightarrow \pi^-\nu_\tau]$  excellently discriminates between Standard–Model and charged–Higgs contributions. By measuring the  $D$  and  $\pi^-$  energies and the angle between the  $D$  and  $\pi^-$  three-momenta one can determine the effective charged–Higgs coupling including a possible CP–violating phase.

### INTRODUCTION

The  $B$  factories BABAR and BELLE have accumulated enough statistics to probe extensions of the Higgs sector of the Standard Model. Notably, the decay  $B^+ \rightarrow \tau^+\nu_\tau$  allows us to place useful constraints on the parameters  $\tan\beta$  and  $M_{H^+}$  of the two–Higgs–doublet model (2HDM) of type II [1]. Here  $\tan\beta$  is the ratio of the two Higgs vacuum expectation values and  $M_{H^+}$  is the mass of the physical charged Higgs boson  $H^+$  in the model. Since the couplings of  $H^+$  to  $b$ 's and  $\tau$ 's grow with  $\tan\beta$ ,  $B^+ \rightarrow \tau^+\nu_\tau$  probes large values of  $\tan\beta$ . Earlier (but less powerful) constraints on the 2HDM were obtained by the OPAL collaboration, which found  $\tan\beta/M_{H^+} < 0.53 \text{ GeV}^{-1}$  from  $\mathcal{B}(\bar{B} \rightarrow X\tau\bar{\nu}_\tau)$  [2] and  $\tan\beta/M_{H^+} < 0.78 \text{ GeV}^{-1}$  from  $\mathcal{B}(\tau \rightarrow \mu\bar{\nu}_\mu\nu_\tau)$  [3] at the 95% CL. The direct search for a charged Higgs boson through  $t \rightarrow bH^+$  at the Tevatron has yielded slightly stronger bounds:  $M_{H^+} > 125 \text{ GeV}$  for  $\tan\beta = 50$  and  $M_{H^+} > 150 \text{ GeV}$  for  $\tan\beta = 70$  [4]. In the low and intermediate  $\tan\beta$  regions, the most constraining bound currently comes from the FCNC–induced process  $b \rightarrow s\gamma$ , which yields  $M_{H^+} > 295 \text{ GeV}$  independently of  $\tan\beta$  [5]. At tree–level the Higgs sector of the Minimal Supersymmetric Standard Model (MSSM) coincides with the type–II 2HDM. The coupling of  $H^+$  to fermions can be modified by a factor of order one due to  $\tan\beta$ –enhanced radiative corrections [6, 7], yet this introduces only a few additional supersymmetric parameters and the access to the Higgs sector in (semi-)leptonic  $B$  decays is not obfuscated like in many other modes, such as the loop–induced  $b \rightarrow s\gamma$  decay. This explains the great theoretical interest in the experimental ranges for  $\mathcal{B}(B^+ \rightarrow \tau^+\nu_\tau)$  [8].

The decay  $B \rightarrow D\tau\nu_\tau$  provides an alternative route to charged–Higgs effects [9–15]. As we will show in the following, this mode is not only competitive with  $B^+ \rightarrow \tau^+\nu_\tau$ , but also opens the door to a potential CP–violating phase in the Yukawa couplings of the  $H^+$  to  $b$  and  $\tau$ .  $B \rightarrow D\tau\nu_\tau$  compares to  $B \rightarrow \tau\nu_\tau$  as follows:

i)  $\mathcal{B}(B \rightarrow D\tau\nu_\tau)$  exceeds  $\mathcal{B}(B \rightarrow \tau\nu_\tau)$  by roughly a factor of 50 in the Standard Model.

ii)  $B \rightarrow D\tau\nu_\tau$  involves the well–known element  $V_{cb}$  of

the Cabibbo–Kobayashi–Maskawa (CKM) matrix. The uncertainty on  $|V_{ub}|$  entering  $B \rightarrow \tau\nu_\tau$  is much larger.

iii)  $\mathcal{B}(B \rightarrow \tau\nu_\tau)$  is proportional to two powers of the  $B$  decay constant  $f_B$ , which must be obtained with non–perturbative methods. Current lattice gauge theory computations are struggling with chiral logarithms and  $f_B^2$  can only be determined with an uncertainty of 30% or more [16].  $B \rightarrow D\tau\nu_\tau$  involves two form factors, one of which can be measured in  $B \rightarrow D\ell\nu_\ell$  ( $\ell = e, \mu$ ) decays [17, 18]. The other one is tightly constrained by Heavy Quark Effective Theory (HQET) [19–22], so that hadronic uncertainties can be reduced to well below 10% once the measurement of  $B \rightarrow D\ell\nu_\ell$  is improved.

iv) Unlike  $B \rightarrow \tau\nu_\tau$  the three–body decay  $B \rightarrow D\tau\nu_\tau$  permits the study of decay distributions which discriminate between  $W^+$  and  $H^+$  exchange [9, 11, 12].

v) The Standard Model (SM) contribution to  $B \rightarrow \tau\nu_\tau$  is (mildly) helicity–suppressed, so that the sensitivity of  $\mathcal{B}(B \rightarrow \tau\nu_\tau)$  to  $H^+$  is enhanced. For  $B \rightarrow D\tau\nu_\tau$  a similar effect only occurs near the kinematic endpoint, where the  $D$  moves slowly in the  $B$  rest frame [9]: While the transversely polarized  $W^+$  contribution suffers from a P–wave suppression, the virtual  $H^+$  recoils against the  $D$  meson in an unsuppressed S–wave.

Items iv) and v) strongly suggest to study differential decay distributions in  $B \rightarrow D\tau\nu_\tau$ . The  $\tau$  in the final state poses an experimental challenge, because it does not travel far enough for a displaced vertex and its decay involves at least one more neutrino. In particular, the  $\tau$  polarization, known as a charged–Higgs analyzer [10], is not directly accessible to experiment. To our knowledge, the only theory papers which address the question of the missing information on the  $\tau$  momentum are [9, 11], where a study of the  $D$  meson energy spectrum is proposed. Another straightforward way to deal with the missing information on the  $\tau$  kinematics, which in addition retains information on the  $\tau$  polarization, is to consider the full decay chain down to the detectable particles stemming from the  $\tau$ . We have studied the decays  $\tau^- \rightarrow \pi^-\nu_\tau$ ,  $\tau^- \rightarrow \rho^-\nu_\tau$ , and  $\tau^- \rightarrow \ell^-\bar{\nu}_\ell\nu_\tau$  and assessed the sensitivity of the decay distributions to  $H^+$  effects. We find that the decay chain

$\bar{B} \rightarrow D\bar{\nu}_\tau\tau^- [\rightarrow \pi^-\nu_\tau]$  discriminates between  $W^+$  and  $H^+$  exchange in an excellent way. In this Letter we present the results for the differential decay rate as a function of the  $D$  and  $\pi^-$  energies and the angle between the  $D$  and  $\pi^-$  three-momenta for this decay chain. Our result greatly facilitates the determination of the effective coupling  $g_S$  governing  $H^+$  exchange, including a potential complex phase, if e.g. a maximum likelihood fit of the data to the theoretical decay distribution given below is employed. A conventional analysis combining Monte Carlo simulations of  $\bar{B} \rightarrow D\bar{\nu}_\tau\tau^-$  and  $\tau^- \rightarrow \pi^-\nu_\tau$  decays would be very cumbersome, because the  $B \rightarrow D\tau\nu_\tau$  differential distributions strongly depend on the a-priori unknown value of  $g_S$ .

### $B \rightarrow D$ FORM FACTORS

The effective hamiltonian describing  $B \rightarrow (D)\tau\nu_\tau$  transitions mediated by  $W^+$  or  $H^+$  reads (with  $q = u(c)$ )

$$H_{\text{eff}} = \frac{G_F}{\sqrt{2}} V_{qb} \{ [\bar{q}\gamma^\mu(1-\gamma_5)b] [\bar{\tau}\gamma_\mu(1-\gamma_5)\nu_\tau] - \frac{\bar{m}_b m_\tau}{m_B^2} \bar{q} [g_S + g_P\gamma_5] b [\bar{\tau}(1-\gamma_5)\nu_\tau] \} + \text{h.c.} \quad (1)$$

The effective coupling constant  $g_P$  only enters the  $B \rightarrow \tau\nu_\tau$  decay, while  $B \rightarrow D\tau\nu_\tau$  is only sensitive to  $g_S$ . The  $B^+$  meson mass  $m_B$  is introduced in Eq. (1), so that  $\mathcal{B}(B \rightarrow \tau\nu_\tau)$  vanishes for  $g_P = 1$ . The above operators as well as  $\bar{m}_b$  are defined in the  $\overline{\text{MS}}$  scheme. In the MSSM, which is our main focus, one has  $g_S = g_P$ .

The analysis of  $B \rightarrow D\tau\nu_\tau$  requires the knowledge of the form factors  $F_V$  and  $F_S$  which parametrize the vector and scalar current matrix elements:

$$\begin{aligned} \langle D(p_D) | \bar{c}\gamma^\mu b | \bar{B}(p_B) \rangle &= F_V(q^2) \left[ p_B^\mu + p_D^\mu - m_B^2 \frac{1-r^2}{q^2} q^\mu \right] \\ &\quad + F_S(q^2) m_B^2 \frac{1-r^2}{q^2} q^\mu, \\ \langle D(p_D) | \bar{c}b | \bar{B}(p_B) \rangle &= \frac{m_B^2(1-r^2)}{\bar{m}_b - \bar{m}_c} F_S(q^2), \end{aligned} \quad (2)$$

where  $p_B$  and  $p_D$  denote the meson four-momenta,  $q = p_B - p_D$ , and  $r = m_D/m_B$ . It is convenient to introduce the normalized form factors  $V_1 \equiv F_V 2\sqrt{r}/(1+r)$  and  $S_1 \equiv F_S(1+r)/(2\sqrt{r})$ , as well as the kinematic variable

$$w \equiv (1+r^2 - q^2/m_B^2)/2r. \quad (3)$$

In the limit of infinitely heavy quark masses  $m_Q = m_b, m_c$  (which are properly infrared-subtracted pole masses), both  $V_1(w)$  and  $S_1(w)$  reduce to the universal Isgur-Wise function  $\xi(w)$ , normalized to  $\xi(1) = 1$ . At the kinematic endpoint  $w = 1$ , corrections to this limit read

$$V_1(1) = \eta_v - \frac{1-r}{1+r} (\delta_{\text{rad}} + \delta_{1/m_Q}), \quad S_1(1) = \eta_v, \quad (4)$$

up to  $\mathcal{O}(\alpha_s^2, 1/m_Q^2)$ . Here  $\eta_v$  denotes radiative corrections in the limit of equal heavy meson masses, and  $\delta_{\text{rad}} (\delta_{1/m_Q})$  are

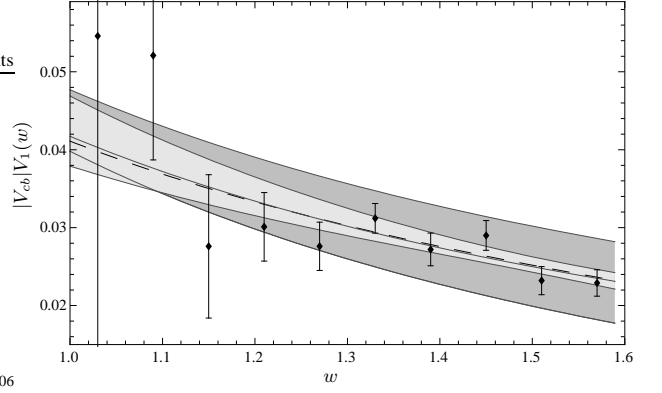


FIG. 1: Vector form factor  $V_1(w)$ . Dots: exp. data [17] with stat. errors only. Dashed: fit to parametrization in [22]. Plain: fit to linear parametrization in [26]. Dark gray band: form factor with HQET constraint at  $w = 1$ ; systematic errors dominate at large recoil. Light gray band: form factor from HFAG [18].

the first order radiative ( $1/m_Q$ ) corrections to the function  $\xi_-$  defined in [20]. The  $\delta_{1/m_Q}$  term depends on the subleading function  $\xi_3(w=1) = \bar{\Lambda}\eta(w=1)$  and on the HQET parameter  $\bar{\Lambda}$ . We take  $\bar{\Lambda} = 0.5 \pm 0.1$  GeV,  $\eta(1) = 0.6 \pm 0.2$  [23],  $\eta_v$  and  $\delta_{\text{rad}}$  to  $\mathcal{O}(\alpha_s)$  from Ref. [24], and add a 5% error to the form factors at  $w = 1$  to account for higher order corrections. We obtain  $V_1(1) = 1.05 \pm 0.08$  and  $S_1(1) = 1.02 \pm 0.05$ .

The semileptonic decay into light leptons  $B \rightarrow D\ell\nu_\ell$  depends solely on the vector form factor  $V_1(w)$ . The measured quantity  $|V_{cb}|V_1(w)$  was fitted by the BELLE collaboration [17] to a two-parameter ansatz  $V_1(w, V_1(1), \rho_1^2)$  [22] derived from dispersion relations and heavy quark spin symmetry [21]. The fitted curve, however, suffers from large statistical and systematic uncertainties:  $|V_{cb}|V_1(1) = (4.11 \pm 0.44 \pm 0.52)\%$ ,  $\rho_1^2 = 1.12 \pm 0.22 \pm 0.14$  [17]. We thus take  $V_1(1)$  from HQET instead, use  $|V_{cb}| = (4.17 \pm 0.07)\%$  from inclusive semileptonic  $B$  decays [25], and only fix the form factor at large recoil  $w = 1.45$  from the data, including the dominant systematic errors in a conservative way:  $|V_{cb}|V_1(1.45) = (2.63 \pm 0.51)\%$ . The form factor over the whole kinematic range is then obtained using a two-parameter description  $F_V(w, a_0^V, a_1^V)$ , which uses a conformal mapping  $w \rightarrow z(w)$  resulting in an essentially linear dependence of  $F_V$  on  $z$  [26]. This linearity in  $z(w)$  is confirmed by the fact that fitting the  $B \rightarrow D\ell\nu_\ell$  data with both  $F_V$  parametrizations without further theoretical constraints essentially gives the same result (see Fig. 1). The sets of parameters corresponding to the minimal and maximal form factors satisfying the HQET constraint at  $w = 1$  are displayed in Tab. I for both parametrizations  $V_1(w, V_1(1), \rho_1^2)$  and  $F_V(w, a_0^V, a_1^V)$ . They delimit the dark gray area in Fig. 1. We stress that the large error band in Fig. 1 at large  $w$  is not due to theory uncertainties but rather to the large systematic error on  $|V_{cb}|V_1(1.45)$  from [17].

We choose to use only the most recent set of experimental data for our numerical analysis. The HFAG [18] treats systematic errors in a different way and, including the older CLEO and ALEPH data, finds smaller uncertainties at large

Parameters	min. $ V_{cb} F$	max. $ V_{cb} F$	centr. $ V_{cb} F$
$\{ V_{cb} V_1(1), \rho_1^2\}$	{0.040, 1.47}	{0.048, 1.06}	{0.044, 1.24}
$ V_{cb} \{a_0^V, a_1^V\}[10^{-5}]$	{0.94, -5.7}	{1.28, -2.2}	{1.11, -3.9}
$ V_{cb} \{a_0^S, a_1^S\}[10^{-4}]$	{1.62, -1.1}	{2.14, -3.2}	{1.88, -6.8}

TABLE I: Parameters  $\{|V_{cb}|V_1(1), \rho_1^2\}$  for  $|V_{cb}|F_V$  [22] and  $\{|V_{cb}|a_0^{V,S}, |V_{cb}|a_1^{V,S}\}$  for  $|V_{cb}|F_{V,S}$  (see [26],  $Q^2 = 0$ ,  $\eta = 2$ , sub-threshold poles:  $m(1^-) = 6.337, 6.899, 7.012$  GeV and  $m(0^+) = 6.700, 7.108$  GeV [29]).  $F_V$  is displayed in dark gray in Fig. 1.

Parameters	min. $ V_{cb} F$	max. $ V_{cb} F$	centr. $ V_{cb} F$
$\{ V_{cb} V_1(1), \rho_1^2\}$	{0.038, 1.01}	{0.047, 1.30}	{0.042, 1.17}
$ V_{cb} \{a_0^V, a_1^V\}[10^{-5}]$	{1.03, -1.3}	{1.17, -4.8}	{1.10, -3.0}
$ V_{cb} \{a_0^S, a_1^S\}[10^{-4}]$	{1.78, -5.7}	{2.00, -7.6}	{1.89, -6.6}

TABLE II: Parameters  $\{|V_{cb}|V_1(1), \rho_1^2\}$  for  $|V_{cb}|F_V$  from HFAG [18], and  $\{|V_{cb}|a_0^{V,S}, |V_{cb}|a_1^{V,S}\}$  for  $|V_{cb}|F_{V,S}$ .  $F_V$  is displayed in light gray in Fig. 1.

recoil (see light gray band in Fig. 1. The corresponding minimal and maximal curves are given in good approximation by the parameters in the first two lines of Tab. II for  $w$  inside the  $B \rightarrow D\tau\nu_\tau$  phase space). The vector form factor has also been studied on the lattice. Computations with quenched Wilson [27] and dynamical staggered [28] fermions, however, both suffer from potentially large systematic errors, which are not fully controlled. In the end, the improvements in the measurements of the  $B \rightarrow D\ell\nu_\ell$  and  $B \rightarrow D\tau\nu_\tau$  modes will go together, and  $|V_{cb}|F_V$  will most likely be best determined from experimental data alone. For the time being, we will proceed with the conservative estimation of Tab. I.

In a similar way, the scalar form factor  $F_S(w, a_0^S, a_1^S)$  is constrained by HQET at  $w = 1$ , while its value at large recoil is fixed from the relation  $F_S(q^2 = 0) = F_V(q^2 = 0)$ . The resulting parameters are displayed in the third line of Tab. I (or Tab. II if  $F_V$  is taken from [18]). As expected from the heavy-quark limit, the normalized form factor  $S_1$  is quite close to  $V_1$  on the whole  $w$  range, with slightly smaller errors.

### CHARGED-HIGGS EFFECTS

The MSSM is a well-motivated new-physics scenario in which charged scalar current interactions occur at tree-level. Resumming the dominant  $\tan\beta$ -enhanced loop corrections to all orders, the couplings  $g_{S,P}$  in Eq. (1) specify to [13, 30]

$$g_S = g_P = \frac{m_B^2}{M_{H^+}^2} \frac{\tan^2\beta}{(1 + \tilde{\epsilon}_0 \tan\beta)(1 + \epsilon_\tau \tan\beta)}. \quad (5)$$

This particular form holds in MSSM scenarios with Minimal Flavor Violation (MFV). The loop factor  $\tilde{\epsilon}_0$  arises from the quark Yukawa sector and depends on ratios of super-particle masses, resulting in a sizable non-decoupling effect  $\tilde{\epsilon}_0 \tan\beta = \mathcal{O}(1)$  for  $\tan\beta = \mathcal{O}(50)$ .  $\epsilon_\tau$  comprises the corresponding effect for the  $\tau$  lepton.  $\tilde{\epsilon}_0$  and  $\epsilon_\tau$  can receive sizable complex phases from the Higgsino mass parameter  $\mu$ , if first-generation sfermions are sufficiently heavy to soften the

impact of the bounds on electric dipole moments on  $\arg\mu$ . Beyond MFV also phases from squark mass matrices will easily render  $g_S$  complex. It is therefore mandatory to constrain – and eventually measure – both magnitude and phase of  $g_S$ . The type-II 2HDM is recovered by setting  $\tilde{\epsilon}_0 = \epsilon_\tau = 0$ .

The  $B \rightarrow D\tau\nu_\tau$  branching ratio has recently been measured by the BABAR collaboration [31]:

$$R^{\text{exp}} \equiv \frac{\mathcal{B}(B \rightarrow D\tau\nu_\tau)}{\mathcal{B}(B \rightarrow D\ell\nu_\ell)} = (41.6 \pm 11.7 \pm 5.2)\%. \quad (6)$$

The normalization to  $\mathcal{B}(B \rightarrow D\ell\nu_\ell)$  reduces the dependence on the vector form factor  $F_V$  and thus tames the main theoretical uncertainties. In the presence of charged-Higgs contributions, the theoretical ratio is approximated to 1% by

$$R^{\text{th}} = \frac{1.126 + 0.037 r_V + r_0^2 (1.544 + 0.082 r_S + N_{H^+})}{10 - 0.95 r_V}, \quad (7)$$

$$N_{H^+} = -r_{cb} \text{Re}[g_S] (1.038 + 0.076 r_S) + r_{cb}^2 |g_S|^2 (0.186 + 0.017 r_S),$$

with  $r_V = (a_1^V/a_0^V)/(-3.4)$ ,  $r_S = (a_1^S/a_0^S)/(-3.5)$ ,  $r_0 = (a_0^S/a_0^V)/17$ , and  $r_{cb} = 0.8/(1 - \overline{m}_c/\overline{m}_b)$ . The dependence on the slope parameters  $a_1^{V,S}$  appears to be quite mild. In Fig. 2 we compare  $R^{\text{th}}$  (right-hand side) as well as  $\mathcal{B}(B \rightarrow \tau\nu)$  (left-hand side) to their one-sigma measurements for positive  $g_S$  and  $g_P$ . For  $R^{\text{th}}$ , we also display the less conservative theoretical prediction obtained from the HFAG vector form factor in Tab. II (light gray band). In particular, we obtain the SM estimates

$$\mathcal{B}(B^- \rightarrow D^0 \tau^- \bar{\nu}_\tau)^{\text{SM}} = (0.71 \pm 0.09)\%$$

and

$$\mathcal{B}(\bar{B}^0 \rightarrow D^+ \tau^- \bar{\nu}_\tau)^{\text{SM}} = (0.66 \pm 0.08)\%.$$

(Error sources:  $|V_{cb}|F_V(w)$ ,  $S_1(1)$ ,  $|V_{cb}|$ ). We cannot reproduce the small errors of Ref. [14].

The  $B \rightarrow D\tau\nu_\tau$  branching fraction is promising to discover – or constrain – charged-Higgs effects, but not to measure  $g_S$  with good precision, as the dependence in Fig. 2 is too flat. The differential distribution in the decay chain  $\bar{B} \rightarrow D\bar{\nu}_\tau\tau^- \rightarrow \pi^-\nu_\tau$  is better suited for that purpose. The experimentally accessible quantities are the energies  $E_D$  and  $E_\pi$  of the  $D$  and  $\pi^-$  mesons, respectively, and the angle  $\theta$  between the three-momenta  $\vec{p}_D$  and  $\vec{p}_\pi$ . We define these quantities in the  $B$  rest frame, which can be accessed from the  $\Upsilon(4S)$  rest frame thanks to full  $B$  reconstruction [31]. We integrate over the phase space of the two unobserved neutrinos in the final state. Our formulae contain the full spin correlation between the production and decay of the  $\tau$ , which is important to discriminate between SM and charged-Higgs contributions. This approach further facilitates the rejection of backgrounds from neutral particles escaping detection, as in  $\bar{B} \rightarrow DD^- \rightarrow \pi^-\pi^0$  with an undetected  $\pi^0$ : If the mass of the undetected particle is  $m$ , this background can be suppressed by cuts excluding the region around

$$\cos\theta = \frac{(m_B - E_D - E_\pi)^2 - 2(E_D^2 - m_D^2) - m^2}{2(E_D^2 - m_D^2)}. \quad (8)$$

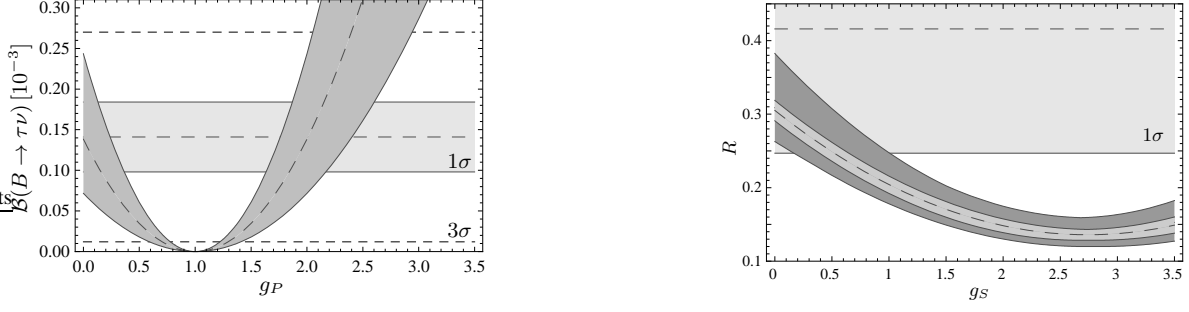


FIG. 2: Left:  $\mathcal{B}(B \rightarrow \tau\nu)$  as a function of  $g_P$ . Light gray band:  $\mathcal{B}^{\text{exp}} = (1.41 \pm 0.43) \times 10^{-4}$  [8]. Gray band:  $\mathcal{B}^{\text{th}}, |V_{ub}| = (3.86 \pm 0.09 \pm 0.47) \times 10^{-3}$  [32], main error from  $B$  decay constant  $f_B = (216 \pm 38)\text{MeV}$  [16]. Right:  $R \equiv \mathcal{B}(B \rightarrow D\tau\nu_\tau)/\mathcal{B}(B \rightarrow D\ell\nu_\ell)$  as a function of  $g_S$ . Light gray band:  $R^{\text{exp}}$ , see (6) [31]. Dark gray band:  $R^{\text{th}}$ , see (7). Gray band:  $R^{\text{th}}$  with the HFAG vector form factor, see Tab. II. SM:  $R^{\text{th}}(g_S = 0) = 0.31^{+0.07}_{-0.05}$  (dark gray) [ $\pm 0.02$  (gray)].

We obtain the differential distribution

$$\frac{d\Gamma(\bar{B} \rightarrow D\bar{\nu}_\tau\tau^- [\rightarrow \pi^-\nu_\tau])}{dE_D dE_\pi d\cos\theta} = G_F^4 f_\pi^2 |V_{ud}|^2 |V_{cb}|^2 \tau_\tau \quad (9)$$

$$\times [C_W(F_V, F_S) - C_{WH}(F_V, F_S) \text{Re}[g_S] + C_H(F_S)|g_S|^2]$$

with form-factor-dependent functions of  $E_D$ ,  $E_\pi$ , and  $\cos\theta$  for the SM ( $C_W$ ), interference ( $C_{WH}$ ), and Higgs ( $C_H$ ) contributions, given as follows for vanishing  $m_\pi$  (this approximation, which is good to 1%, is not used in our numerical analysis),

$$C_W = \kappa \frac{m_\tau^4}{2} \frac{l^2}{p_\pi \cdot l} \left\{ P^2(b-1) + (P \cdot l)^2 \frac{2b}{l^2} + \left[ \frac{l^2(P \cdot p_\pi)^2}{(p_\pi \cdot l)^2} - \frac{2(P \cdot l)(P \cdot p_\pi)}{p_\pi \cdot l} \right] (3b-1) \right\}, \quad (10)$$

$$C_{WH} = 2\kappa m_\tau^4 \frac{(1-r^2)F_S}{1-\bar{m}_c/\bar{m}_b} b \left[ P \cdot l - \frac{l^2 P \cdot p_\pi}{p_\pi \cdot l} \right],$$

$$C_H = \kappa m_\tau^6 \frac{(1-r^2)^2 F_S^2}{(1-\bar{m}_c/\bar{m}_b)^2} \left( 1 - \frac{m_\tau^2}{2p_\pi \cdot l} \right),$$

where  $\bar{m}_c$  and  $\bar{m}_b$  must be evaluated at the same scale so that  $\bar{m}_c/\bar{m}_b = 0.20 \pm 0.02$  [33], and

$$P = F_V(p_B + p_D) - (F_V - F_S) \frac{m_B^2(1-r^2)}{q^2} (p_B - p_D),$$

$$\kappa = \frac{E_\pi \sqrt{E_D^2 - m_D^2}}{128 \pi^4 m_B m_\tau}, \quad b = \frac{m_\tau^2}{p_\pi \cdot l} \left( 1 - \frac{m_\tau^2}{2p_\pi \cdot l} \right),$$

$$l = p_B - p_D - p_\pi, \quad q^2 = (p_B - p_D)^2. \quad (11)$$

The dot products appearing in Eqs. (10) and (11) are related to the energies, momenta, and the angle  $\theta$  measured in the  $B$  rest frame as  $p_B \cdot l = m_B(m_B - E_D - E_\pi)$ ,  $p_D \cdot l = E_D(m_B - E_D - E_\pi) + |\vec{p}_D|^2 + |\vec{p}_D|E_\pi \cos\theta$ ,  $p_\pi \cdot l = E_\pi(m_B - E_D) + |\vec{p}_D|E_\pi \cos\theta$ , and  $p_B \cdot p_D = m_B E_D$ . Further  $\tau_\tau = (290.6 \pm 1.0) \times 10^{-15} \text{s}$  is the  $\tau$  lepton lifetime,  $f_\pi = (130.7 \pm 0.1 \pm 0.36) \text{MeV}$  the pion decay constant, and the CKM matrix elements are  $|V_{ud}| = 0.97377 \pm 0.00027$  and  $|V_{cb}| = (41.7 \pm 0.7) \times 10^{-3}$ , the latter being well determined from inclusive semileptonic  $B$  decays [25]. Remarkably, one can probe a CP-violating phase of  $g_S$  by exploiting the shape

of the distribution in Eq. (9), which is not possible from the branching fraction of either  $B \rightarrow D\tau\nu_\tau$  or  $B \rightarrow \tau\nu_\tau$ .

For illustration, we show the differential decay distribution including charged-Higgs effects in comparison with the SM for the meson energies  $E_D = 2 \text{ GeV}$  and  $E_\pi = 1 \text{ GeV}$ , so that the whole range of  $\cos\theta$  is kinematically accessible. In this particular region of phase space the SM rate is strongly suppressed for  $\cos\theta = -1$ . For a large scalar coupling  $g_S = 2$  (Fig. 3, left), the Higgs contribution dominates the rate at this point (dark gray band), so that we can clearly distinguish it from the SM (light gray band). The experimental information from  $\mathcal{B}(B \rightarrow \tau\nu_\tau)$  constrains  $|1 - g_P|$ . For real  $g_P$  this permits a range near  $g_P = 0$  and another range around  $g_P = 2$ . In the MSSM situation with  $g_P = g_S$ , the case  $g_S = 2$  therefore is in agreement with  $B \rightarrow \tau\nu_\tau$ , but can be confirmed or ruled out by measuring our distribution. The discrimination potential for the phase of  $g_S$  shows up in the light gray band: It corresponds to a complex  $g_S = 1 + i$ , which yields the same  $\mathcal{B}(B \rightarrow \tau\nu_\tau)$  as  $g_S = 0, 2$ . The  $B \rightarrow D\tau\nu_\tau$  branching ratio alone may also help to distinguish between these solutions, depending on the future experimental value of  $\mathcal{B}(B \rightarrow D\tau\nu_\tau)$ , see Fig. 2. For general  $g_S$  values, a fit to the triple differential distribution in Eq. (9) would excellently quantify charged-Higgs effects, especially once better experimental information on the form factors is available, as we illustrate with fixed  $D$  and  $\pi^-$  energies in Fig. 3 (right-hand side) for  $g_S = 0.5$ . Such a fit would combine information from different parts of the phase space, and thus resolve much smaller  $g_S$  values. A more precise quantitative analysis would require the fit to actual data, and thus goes beyond the scope of this paper. Still, keep in mind that even with more precise  $B \rightarrow \tau\nu_\tau$  experimental data and improved estimates of  $f_B$  and  $|V_{ub}|$ , a value of  $g_P \simeq 0.2 - 0.3$  will be very difficult to exclude with  $\mathcal{B}(B \rightarrow \tau\nu_\tau)$ .  $B \rightarrow D\tau\nu_\tau$  is thus definitely competitive.

As mentioned in the Introduction, a similar analysis was performed for the other  $\tau$  decay channels  $\tau^- \rightarrow \rho^- \nu_\tau$  and  $\tau^- \rightarrow \ell^- \bar{\nu}_\ell \nu_\tau$ , which together with  $\tau^- \rightarrow \pi^- \nu_\tau$  constitute more than 70% of the  $\tau$  branching fraction. Ultimately, a combined analysis of all these modes is desirable in order to exploit the available and forthcoming experimental data in an optimal way.

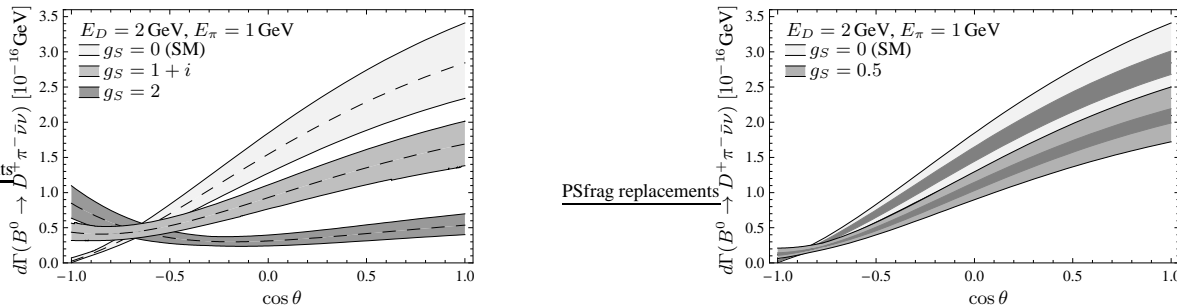


FIG. 3:  $\bar{B}^0 \rightarrow D^+ \bar{\nu}_\tau \tau^- [\rightarrow \pi^- \nu_\tau]$  angular distribution for  $E_D = 2$  GeV and  $E_\pi = 1$  GeV. Left:  $g_S = 0, 1 + i, 2$ . Right:  $g_S = 0, 0.5$  (dark gray: without uncertainties in  $F_V(w)$  and  $V_{cb}$ , errors from  $S_1(1)$  and  $\bar{m}_c/\bar{m}_b$ ). The conservative form factor estimates of Tab. I were considered.

## CONCLUSIONS

We have studied charged–Higgs effects in a differential distribution of the decay chain  $\bar{B} \rightarrow D \bar{\nu}_\tau \tau^- [\rightarrow \pi^- \nu_\tau]$ , which has the following advantages over the branching fractions  $\mathcal{B}(B \rightarrow \tau \nu_\tau)$  and  $\mathcal{B}(B \rightarrow D \tau \nu_\tau)$ :

i) The Higgs coupling constant  $g_S$  can be determined from the *shape* of the distribution in sensitive phase space regions. This analysis should be possible with current  $B$  factory data.

ii) The dependence on both  $|g_S|$  and  $\text{Re}[g_S]$  allows to quantify a possible CP–violating phase. Since our decay distribution is a CP–conserving quantity, the phase of  $g_S$  is determined with a two–fold ambiguity. In the MSSM such a phase stems from the  $\mu$  parameter or the soft breaking terms and enters through  $\tan\beta$ –enhanced loop factors.  $B \rightarrow D \tau \nu$  complements collider studies of these phases [34].

The main uncertainties stem from the form factors. One can gain a much better accuracy with better data on the vector form factor  $F_V$ . The recent  $B \rightarrow D \ell \nu_\ell$  measurement by BABAR [35] furnishes promising data for a new fit.

Within the MSSM, one will be able to place new constraints on the  $\tan\beta - M_{H^\pm}$  plane, once our results are confronted with actual data from the  $B$  factories. If  $\tan\beta/M_{H^\pm}$  is indeed large, there is a fair chance to reveal charged–Higgs effects ahead of the LHC.

*Acknowledgments:* The authors acknowledge helpful discussions with Richard Hill and Michael Feindt. This work is supported in part by the DFG grant No. NI 1105/1–1, by the DFG–SFB/TR9, and by the EU Contract No. MRTN-CT-2006-035482, “FLAVIANet”.

[1] W. Hou, Phys. Rev. D **48**, 2342 (1993).  
 [2] OPAL Collaboration, Phys. Lett. B **520**, 1 (2001).  
 [3] OPAL Collaboration, Phys. Lett. B **551**, 35 (2003).  
 [4] J. Nielsen [CDF and D0 Collaborations], Nucl. Phys. Proc. Suppl. **177**, 224 (2008).  
 [5] M. Misiak *et al.*, Phys. Rev. Lett. **98**, 022002 (2007).  
 [6] L. Hall, R. Rattazzi and U. Sarid, Phys. Rev. D **50**, 7048 (1994); T. Blazek, S. Raby and S. Pokorski, Phys. Rev. D **52**, 4151 (1995). M. Carena *et al.*, Nucl. Phys. B **577**, 88 (2000). For

earlier work on  $t \rightarrow bH^+$  without resummation of  $\tan\beta$ –enhanced radiative corrections, see R.A. Jimenez and J. Sola, Phys. Lett. B **389**, 53 (1996).  
 [7] A. Akeroyd and S. Recksiegel, J. Phys. G **29**, 2311 (2003).  
 [8] BELLE Collaboration, Phys. Rev. Lett. **97**, 251802 (2006); BABAR Collaboration, Phys. Rev. D **76**, 052002 (2007); average: D. Monorchio, talk presented at HEP2007, <http://www.hep.man.ac.uk/HEP2007/>.  
 [9] B. Grzadkowski and W. Hou, Phys. Lett. B **283**, 427 (1992).  
 [10] M. Tanaka, Z. Phys. C **67**, 321 (1995).  
 [11] K. Kiers and A. Soni, Phys. Rev. D **56**, 5786 (1997).  
 [12] T. Miki, T. Miura and M. Tanaka, [hep-ph/0210051].  
 [13] H. Itoh, S. Komine and Y. Okada, Prog. Theor. Phys. **114**, 179 (2005).  
 [14] C.-H. Chen and C.-Q. Geng, JHEP **0610**, 053 (2006).  
 [15] J.F. Kamenik and F. Mescia, [0802.3790][hep-ph].  
 [16] M. Della Morte, PoS LAT2007, 8.  
 [17] BELLE Collaboration, Phys. Lett. B **526**, 258 (2002).  
 [18] Heavy Flavor Averaging Group, [0704.3575][hep-ex], and online update at <http://www.slac.stanford.edu/xorg/hfag/>.  
 [19] N. Isgur and M.B. Wise, Phys. Lett. B **232**, 113 (1989); **237**, 527 (1990); B. Grinstein, Nucl. Phys. B **339**, 253 (1990); E. Eichten and B. Hill, Phys. Lett. B **234**, 511 (1990); H. Georgi, Phys. Lett. B **240**, 447 (1990).  
 [20] M. Neubert, Phys. Rept. **245**, 259 (1994).  
 [21] C.G. Boyd, B. Grinstein and R.F. Lebed, Phys. Rev. D **56**, 6895 (1997).  
 [22] I. Caprini, L. Lellouch and M. Neubert, Nucl. Phys. B **530**, 153 (1998).  
 [23] Z. Ligeti, Y. Nir and M. Neubert, Phys. Rev. D **49**, 1302 (1994).  
 [24] M. Neubert, Phys. Rev. D **46**, 2212 (1992).  
 [25] W.-M. Yao *et al.* [Particle Data Group], J. Phys. G **33**, 1 (2006).  
 [26] R. Hill, [hep-ph/0606023].  
 [27] G. M. de Ditiis, R. Petronzio and N. Tantalo, JHEP **0710**, 062 (2007).  
 [28] M. Okamoto *et al.*, Nucl. Phys. Proc. Suppl. **140**, 461 (2005).  
 [29] E. Eichten and C. Quigg, Phys. Rev. D **49**, 5845 (1994).  
 [30] A. Buras *et al.*, Nucl. Phys. B **659**, 3 (2003).  
 [31] BABAR Collaboration, Phys. Rev. Lett. **100**, 021801 (2008).  
 [32] CKMfitter, fit inputs for summer 2007, <http://www.slac.stanford.edu/xorg/ckmfitter/>.  
 [33] K. Chetyrkin, J. Kühn and M. Steinhauser, Comput. Phys. Commun. **133**, 43 (2000). Input values: J. Kühn, M. Steinhauser and C. Sturm, Nucl. Phys. B **778**, 192 (2007).  
 [34] A. Bartl, K. Hohenwarter-Sodek, T. Kernreiter, O. Kittel and M. Terwort, [0802.3592][hep-ph], and references therein.  
 [35] BABAR Collaboration, [0708.1738][hep-ex].